

**Figure 1** | Classical and non-classical nucleation pathways from solution. **a**, Cryo-TEM image showing the attachment of primary particles (arrows) to a magnetite nanoparticle. **b**, Nucleation pathways from ions and clusters of ions to the bulk crystal. Both clusters and free ions can nucleate the crystalline bulk phase either directly or through an amorphous precursor phase. **c**, Schematic of the excess free-energy of clusters, relative to the free ions in solution and normalized to the bulk surface energy, as a function of the average cluster size. Hypothetical local minima would correspond to metastable clusters, whereas stable clusters (which by definition should have lower free-energy than the free ions) would correspond to the absolute minimum. **d**, Dependence of the boundary between the direct and indirect pathways on both the supersaturation and surface energy of the amorphous precursor phase relative to the corresponding values for the crystalline phase. When the relative supersaturation of the amorphous phase is small or the relative surface energy is large, the crystalline phase nucleates directly. As the relative supersaturation of the amorphous phase is increased or its surface energy decreases, the formation of the crystalline phase through an indirect pathway becomes favourable. The boundary shifts towards higher surface energy and lower supersaturation when metastable clusters are the source of nucleation, making the indirect pathway more likely. Instead, when clusters are stable, the boundary shifts in the opposite direction, thus favouring the direct pathway. Figure reproduced with permission from: **a,b,d**, ref. 5, © 2013 NPG; **c**, ref. 6, © 2012 RSC.

population created through thermal fluctuations that provide a low-barrier path to nucleation. In the latter, they are more stable than the free ions and can never lie on the thermodynamically favoured path; hence, nucleation by stable clusters can only dominate for kinetic reasons. Either way, as the analysis of Baumgartner *et al.* makes clear, there is no single pathway to the crystalline state, and the thermodynamically favoured pathway depends on many factors.

Each of the non-classical scenarios makes a clear prediction about the size distribution of clusters and its evolution with time. For example, the average size of liquid droplets formed through spinodal decomposition should grow with time whereas clusters occupying free-energy minima should maintain a constant size distribution. Therefore, resolution of the controversy over classical versus non-classical pathways via metastable versus stable clusters, and distinguishing solid-phase clusters that occupy free-energy minima from the products of spinodal decomposition can, in principle, be achieved by measuring particle-size distributions. Although no method can yet deliver the definitive dataset, recent advances in fluid-based TEM and free-electron-laser X-ray scattering may soon enable us to fill this knowledge gap and finally establish a predictive model of nucleation. □

Jim De Yoreo is at the Pacific Northwest National Laboratory, Richland, Washington 99352, USA. e-mail: james.deyoreo@pnnl.gov

#### References

- Gebauer, D., Volkel, A. & Cölfen, H. *Science* **322**, 1819–1822 (2008).
- Pouget, E. M. *et al.* *Science* **323**, 1455–1458 (2009).
- Habraken, W. J. E. M. *et al.* *Nature Commun.* **4**, 1507 (2013).
- Van Driessche, A. E. S. *et al.* *Science* **336**, 69–72 (2012).
- Baumgartner, J. *et al.* *Nature Mater.* **12**, 310–314 (2013).
- Hu, Q. *et al.* *Faraday Discuss.* **159**, 509–523 (2012).
- Raiteri, P. & Gale, J. D. *J. Am. Chem. Soc.* **132**, 17623–17634 (2010).
- Navrotsky, A. *Proc. Natl Acad. Sci. USA* **101**, 12096–12101 (2004).
- Bewernitz, M. A., Gebauer, D., Long, J., Cölfen, H. & Gower, L. B. *Faraday Discuss.* **159**, 291–312 (2012).
- Galkin, O., Chen, K., Nagel, R. L., Hirsch, R. E. & Vekilov, P. G. *Proc. Natl Acad. Sci. USA* **99**, 8479–8483 (2002).

## BIOIMAGING

# Illuminating the deep

Three-photon imaging enables deeper tissue penetration *in vivo*, however, a lack of imaging probes has restricted its use. Now, this problem has been overcome by engineering non-toxic manganese-doped quantum dots.

Kyryl Zagorovsky and Warren C. W. Chan

Optical imaging aims to produce a picture of the activities of biological molecules, cells and tissues. This is achieved by tagging biological components with different emitting fluorescent probes,

and observing their unique colours to identify the multitude of biological activities with exquisite single-molecule sensitivity<sup>1,2</sup>. The emitting signal can be generated by one-, two- or three-photon

excitation (Fig. 1). Imaging based on a one-photon process is most common because of the availability of optical probes, excitation sources and simpler instrumentation set-up, but three-photon imaging can yield

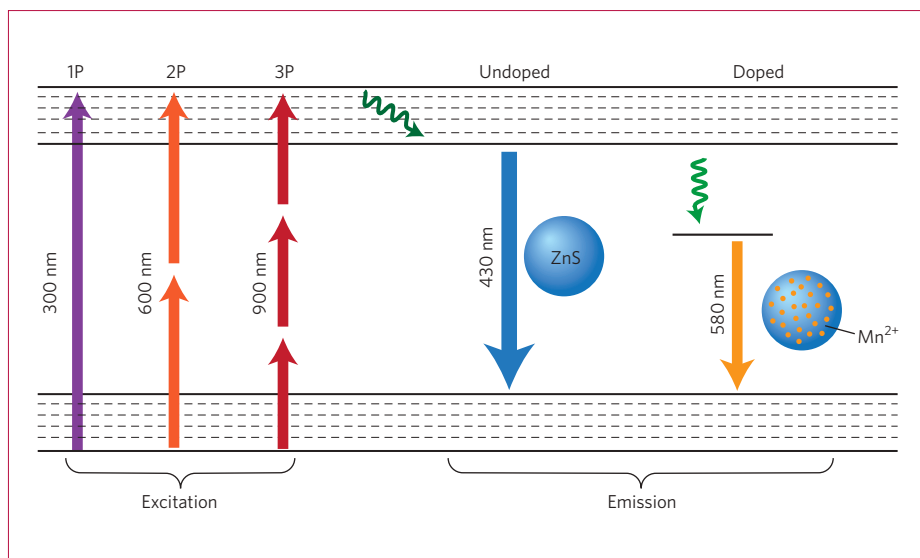


**Figure 1** | A Jablonski diagram comparing one-, two- and three-photon fluorescence of quantum dots. Each electron can be excited by a single energetic 300-nm photon (one photon, 1P), two 600-nm photons (two photon, 2P), or three 900-nm photons (three photon, 3P). Three-photon fluorescence allows the quantum dots to be excited in the near-IR low tissue interference region. Normal fluorescence emission from ZnS quantum dots is near 430 nm. Doping ZnS with Mn<sup>2+</sup> metal redshifts the emission to 580 nm, reducing tissue absorbance and scattering of emitted light.

the deepest tissue penetration, improved resolution, highest sensitivity, and minimal photodamage and photobleaching<sup>3</sup> (Fig. 2). Despite these advantages, a major limitation of three-photon imaging is the lack of available probes because most have very small three-photon cross-sections and low quantum efficiencies. A small cross-section suggests that few electrons can transition to the excited state, leading to a small number of electrons generating photons when they relax to the ground state, resulting in a dim fluorescence signal. The two- and three-photon cross-sections of ZnS-capped CdSe quantum dots, and ZnS and ZnSe quantum dots, however, are orders of magnitude higher than most organic dye molecules, making quantum dots excellent probes for multiphoton microscopy<sup>4–6</sup>. There is some controversy, however, surrounding the toxicity of cadmium-containing quantum dots<sup>7</sup> and the inability of the ultraviolet-to-blue emissions from the ZnS and ZnSe quantum dots to escape body tissue. As a result, the development of quantum dots for *in vivo* multiphoton imaging is limited.

Now, writing in *Nature Materials*, Hyeon and co-workers avoid the toxicity debate by developing a biocompatible manganese-doped ZnS quantum dot probe with four orders-of-magnitude larger three-photon absorption cross-section than common ultraviolet fluorescent dyes<sup>8</sup>. Importantly, the manganese did not

affect the cross-section but redshifted the emission wavelength of the ZnS quantum dots to the orange, thus enabling more light to emanate from the tissues. Moreover, they show the application of three-photon excitation of these quantum dots to image and target cells *in vitro* and *in vivo*.

This study by Hyeon and co-workers shows the potential benefits of optical techniques for imaging diseased cells and tissues in live animals and patients. It has been speculated that optical imaging can colour code the molecular variability and

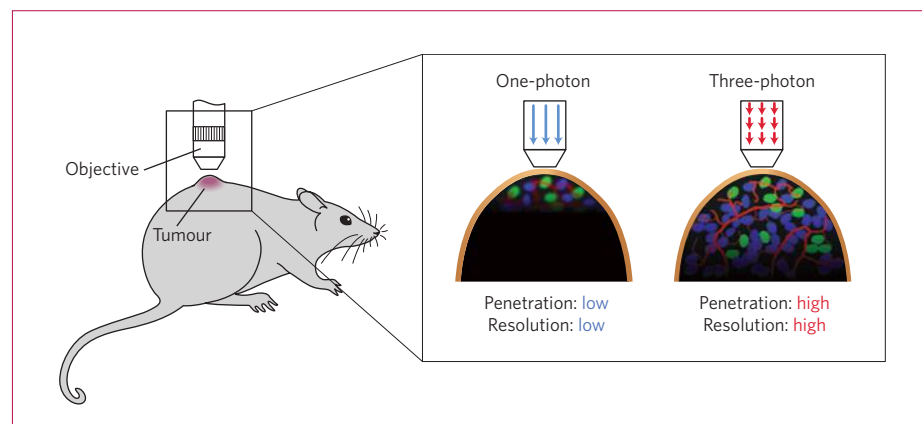


**Figure 2** | Three-photon fluorescence microscopy improves tissue penetration depth and resolution *in vivo*. A tumour can be imaged directly through the skin in a live animal, however, the optical imaging modality (that is, one- or three-photon) and properties of the probes will determine the imaging penetration depth and resolution. If multiple tissue components are labelled with different colour dyes, it is possible to image them simultaneously.

heterogeneity of diseased tissues *in vivo*, which could improve diagnostic accuracy and simplify image-guidance for surgical resection<sup>9</sup>. Towards this objective, in the past, researchers have focused on one-photon near-infrared (IR) optical probes because this wavelength window (650–950 nm) has low tissue interference and will yield a higher optical signal and penetration depth for animal imaging than ultraviolet or visible probes<sup>10</sup>. There are, however, limited near-IR emitting biocompatible probes with good stability and quantum efficiency. Theoretically it has been speculated that imaging down to 1–2 cm may be possible<sup>11</sup>, but only a penetration depth of ~60 μm has been achieved experimentally, which limits clinical imaging to the immediate surface layer of the tissue<sup>12</sup>. Now, Hyeon and co-workers show that the use of three-photon excitation of Mn-doped ZnS quantum dots can improve the imaging depth by a factor of two. This is achieved by redshifting the fluorescence of ZnS-quantum dots and excitation with a deep-penetrating near-IR 920-nm laser to reduce some of the optical interference from tissues (Fig. 1).

Coincidentally, it has been shown recently that improvements in three-photon microscope design can lead to an imaging depth of 1,300 μm (ref. 13). Combining the probe development of Hyeon and co-workers with this more sophisticated microscope technology should allow an experimental penetration depth of ~3 mm. Although this is still poor compared with magnetic resonance imaging<sup>14</sup>, the results show that it is possible to achieve greater imaging depth by manipulating the fluorescence processes and instrumental set-up.

In addition to the enhanced three-photon cross-section, the Mn-doped quantum dots can be encapsulated in phospholipid shells, which allows them to be conjugated to targeting agents. The optical signal from the quantum dots identified the location of the targeting agent, and subsequently the cell receptors. Hyeon and co-workers demonstrate that a LyP-1 peptide coated onto the surface of the quantum dots could target the p32 receptors on MDA-MB-435 tumour cells in culture, and further show the targeting of  $\alpha_v\beta_3$  receptors on tumour vascular cells in a xenograft mouse model by a surface-immobilized RGD peptide. These quantum dots are less toxic in culture in comparison with ZnS-capped CdSe, and CdSe quantum dots because a higher dose of Mn-doped quantum dots was required to kill the cells. Histopathology findings combined with liver and kidney biomarker analysis showed no *in vivo* toxicity after the injection of 100  $\mu$ l of 40 nmol Mn-doped ZnS quantum dots. The results clearly show that these quantum dots are biocompatible, can be conjugated to targeting agents and are safer than Cd-based quantum dots.

Optical microscopy techniques are the dominant imaging modality for analysing cells and tissues *in vitro*. For *in vivo*

clinical applications, however, optical imaging techniques are minimally used because of limited penetration depth and poor signal-to-noise ratio (Fig. 2). Many diseased tissues are typically deeper than 3 mm and therefore, there is a need to further improve the design of probes and instruments for this imaging modality to compete in clinical applications. One advantage of optical imaging over other imaging techniques is the ability to detect the molecular heterogeneity of diseases. Bioengineers are using various molecular biology techniques to identify homing molecules to target contrast agents and therapeutics to diseased tissues based on the unique receptor expression profiles<sup>10</sup>. By using multiple labels on different receptors, one could envisage the colour coding of diseases, which cannot be achieved by using magnetic or radio imaging. Apart from improving the optical imaging depth, there is also a need to enhance the delivery efficiency of nanoparticles to the diseased site and to engineer them to be eliminated from the body to mitigate the issues of long-term toxicity through repeated dosing<sup>15</sup>. Although optical imaging is an excellent technique for use in research, significant effort is required to advance this

imaging modality for routine patient care and diagnostics. □

Kyryl Zagorovsky and Warren C. W. Chan are in the Institute of Biomaterials and Biomedical Engineering, Terrence Donnelly Centre for Cellular and Biomolecular Research, Department of Chemical Engineering, Materials Science and Engineering, and Chemistry, 160 College Street, Room 450, Toronto, Ontario M5S 3E1, Canada.  
e-mail: warren.chan@utoronto.ca

#### References

1. Pepperkok, R. & Ellenberg, J. *Nature Rev. Mol. Cell Biol.* **7**, 690–696 (2006).
2. Joo, C., Balci, H., Ishitsuka, Y., Buranachai, C. & Ha, T. *Annu. Rev. Biochem.* **77**, 51–76 (2008).
3. Zipfel, W. R., Williams, R. M. & Webb, W. W. *Nature Biotechnol.* **21**, 1369–1377 (2003).
4. Larson, D. R. *et al. Science* **300**, 1434–1436 (2003).
5. Lad, A. M., Kiran, P. P., Kumar, G. R. & Mahamuni, S. *Appl. Phys. Lett.* **90**, 133113 (2007).
6. Feng, X. *et al. Opt. Express* **16**, 6999–7005 (2008).
7. Yong, K. T. *et al. Chem. Soc. Rev.* **42**, 1236–1250 (2013).
8. Yu, J. J. *et al. Nature Mater.* **12**, 359–366 (2013).
9. Frangioni, J. V. *Curr. Opin. Chem. Biol.* **7**, 626–634 (2003).
10. Luo, S., Zhang, E., Su, Y., Cheng, T. & Shi, C. *Biomaterials* **32**, 7127–7138 (2011).
11. Smith, A. M., Mancini, M. C. & Nie, S. *Nature Nanotech.* **4**, 710–711 (2009).
12. Centonze, V. E. & White, J. G. *Biophys. J.* **75**, 2015–2024 (1998).
13. Horton, N. G. *et al. Nature Photon.* **7**, 205–209 (2013).
14. Blamire, A. M. *Br. J. Radiol.* **81**, 601–617 (2008).
15. Albanese, A., Tang, P. S. & Chan, W. C. W. *Annu. Rev. Biomed. Eng.* **14**, 1–16 (2012).

## GRANULAR MATERIALS

# Highly evolved grains

By efficiently exploring the huge variety of possible grain shapes, computer algorithms that mimic evolution make possible the design of grains that pack into configurations with the desired mechanical or structural properties.

Corey S. O'Hern and Mark D. Shattuck

**B**iological systems are highly optimized through genetic mutation, reproduction and evolution. For example, the interactions between amino acid side-chains have been exquisitely fine tuned so that proteins can reliably fold and bind within cells to orchestrate all of the necessary cellular functions. Can such an optimization process be applied to designing robust, more energy-efficient and less-costly materials? The task is daunting. For each material, there are a vast number of possible combinations of microstructural variables, and the complex relationship between microstructure and bulk properties is in most cases not known. Therefore, traditional approaches to materials design are often trial-and-error combinatorial searches through high-dimensional parameter spaces.

Algorithms based on evolution — such as genetic algorithms — show great promise in solving such problems<sup>1</sup>, where the complex relationships between the myriad microscale variables and the properties to be optimized are not known *a priori*. Reporting in *Nature Materials*, Marc Miskin and Heinrich Jaeger employed a genetic algorithm to optimize the mechanical properties of granular materials<sup>2</sup>. Granular media are ubiquitous in nature and industrial contexts; examples include the Earth's crust, pharmaceutical powders and agricultural products. Granular media are also used in composite materials to enhance strength, as in concrete, or acoustic properties, as in phononic metamaterials<sup>3,4</sup>. They are far-from-equilibrium systems, as they are too large to experience thermal fluctuations

and thus must be externally driven to induce particle motion. Also, because traditional approaches based on statistical mechanics often fail to describe them, the design of granular materials poses particular difficulties.

Miskin and Jaeger sought to maximize the strength (elastic modulus) of static granular packings as a function of the possible shapes of the constituent grains. The researchers considered composite grains formed from two to five equal-sized spherical particles that can be rigidly connected into all possible non-branched shapes. Their genetic algorithm is able to efficiently identify the particle shapes that give rise to the stiffest (a compact shape) and softest (rod-like shape) packings (Fig. 1). Moreover, the authors used their algorithm to search for particle shapes